

Carbon nanofiber supported cobalt catalysts for Fischer–Tropsch synthesis with high activity and selectivity

Zhixin Yu,^a Øyvind Borg,^a De Chen,^a Bjørn Christian Enger,^a Vidar Frøseth,^a Erling Rytter,^b
Hanne Wigum,^b and Anders Holmen^{a,*}

^aDepartment of Chemical Engineering, Norwegian University of Science and Technology (NTNU), Trondheim N-7491, Norway

^bStatoil R&D, Postuttak, Trondheim N-7005, Norway

Received 5 February 2006; accepted 24 February 2006

Platelet and fishbone carbon nanofibers (CNFs) have been used as supports for cobalt Fischer–Tropsch catalysts. The activity and selectivity of the CNF supported catalysts have been studied at 483 K, 20 bar, and H₂/CO = 2.1, and compared with corresponding activity and selectivity for α -Al₂O₃ and γ -Al₂O₃ supported cobalt catalysts. The platelet CNF supported catalyst has demonstrated high activity and high selectivity to C₅₊ hydrocarbons, with activity comparable with Co/ γ -Al₂O₃ and selectivity comparable with Co/ α -Al₂O₃.

KEY WORDS: carbon nanofibers; catalyst support; Fischer–Tropsch synthesis.

1. Introduction

Gas-to-liquid technologies have become increasingly important during the last years. Fischer–Tropsch synthesis is a promising route for production of liquid fuels from natural gas. A crucial element in the Fischer–Tropsch synthesis is the development of active catalysts with high wax selectivity. Cobalt is the preferred catalyst for the Fischer–Tropsch synthesis based on natural gas derived synthesis gas because of its high activity and selectivity and low water–gas shift activity. Different supports have been used for cobalt catalysts, including alumina, silica and titania [1–4]. Normally, high catalyst activity, slow deactivation rates, high C₅₊ selectivity and high mechanical strength are the most critical design criteria in the choice of Fischer–Tropsch catalysts.

Cobalt supported on γ -Al₂O₃ has been considered as a suitable catalyst for the synthesis of hydrocarbons via the Fischer–Tropsch synthesis [5]. Recently, Eri *et al.* [6] obtained significantly higher C₅₊ selectivity by using cobalt supported on low surface area α -Al₂O₃ (15 m²/g). However, a main drawback of α -Al₂O₃ as a support for the Fischer–Tropsch synthesis is the low cobalt loading and dispersion achieved during incipient wetness impregnation. The reaction rate (g/(g_{cat} · h)) of α -Al₂O₃ supported cobalt catalysts is therefore lower than that of Co/ γ -Al₂O₃, although the selectivity is higher.

Recently, carbon nanofibers (CNFs) have been found to be interesting supports for a number of catalytic reactions [7], and both Fe and Co based

Fischer–Tropsch catalysts supported on CNFs have been reported [8, 9]. Particularly, Bezemer *et al.* [9] have demonstrated that CNFs could be a promising support for the Fischer–Tropsch synthesis with good activity and selectivity. However, the Fischer–Tropsch reaction has been studied mostly at atmospheric pressures.

In this study, CNFs with two different structures, namely, fishbone and platelet, have been prepared and used as the supports for cobalt based Fischer–Tropsch catalysts. The catalysts have been studied at 20 bar and the results were compared with α -Al₂O₃ and γ -Al₂O₃ supported cobalt catalysts.

2. Experimental

The synthesis of CNFs with fishbone and platelet structure was performed according to a method described previously [10]. The as-synthesized CNFs were boiled in concentrated nitric acid for 1 h to remove metal impurities and introduce surface oxygen groups. All the cobalt catalysts used in this study were prepared by standard one-step incipient wetness method with an aqueous solution of cobalt nitrate hexahydrate, and the cobalt loading is always 12 wt.%. α - and γ -Al₂O₃ supported cobalt catalysts were prepared for comparison. The catalysts were dried at 393 K for 3 h in an oven. The CNFs supported catalysts were calcined at 573 K in flowing nitrogen for 6 h and the alumina supported catalysts were calcined at 573 K for 16 h in flowing air.

The surface area and pore characteristics of the different catalysts have been determined by nitrogen adsorption/desorption measurements using a Microm-

*To whom correspondence should be addressed.
E-mail: holmen@chemeng.ntnu.no

eritics TriStar 3000 apparatus. The pore volume of Co/ α -Al₂O₃ was determined by mercury intrusion using a Carlo Erba Porosimeter 2000 unit. X-ray diffraction (XRD) analysis was carried out at room temperature with a Siemens D5005 X-ray diffractometer using CuK α radiation. The particle sizes were calculated from the Scherrer equation by assuming a *K* factor of 1. Hydrogen chemisorption was performed at 313 K with a Micromeritics ASAP 2010 apparatus. TEM study was performed using a JEOL 2010F electron microscope equipped with a field emission gun. TEM specimens were prepared by ultrasonic dispersion of the grounded catalyst samples in ethanol, and then a drop of the suspension was applied to a holey carbon copper grid.

Fischer–Tropsch synthesis was performed in a fixed-bed reactor (stainless steel, 10 mm inner diameter). A detailed description of the reaction set-up is given elsewhere [11]. The catalyst (1.7 g) was diluted with inert silicon carbide particles (4.0 g, 75–150 μ m). The sample was reduced *in situ* in hydrogen at ambient pressure while the temperature was increased at 1 K/min to 623 K. After 16 h of reduction, the catalyst was cooled to 443 K. The system was then pressurised to 20 bar and synthesis gas of molar ratio H₂/CO = 2.1 was introduced to the reactor. The temperature was then gradually increased to 483 K. The C₅₊ selectivity was calculated by subtracting the amount of C₁–C₄ hydrocarbons and carbon dioxide in the product gas mixture from the total mass balance. The activity is reported as the hydrocarbon formation rate (g/(g_{cat} · h)).

3. Results and discussion

3.1. Catalyst characterization

Mercury intrusion measurement shows that Co/ α -Al₂O₃ has a low surface area of 9 m²/g and a pore volume of 0.25 cm³/g. It is worth noting that α -Al₂O₃ contains macropores that contribute to the overall pore volume. Nitrogen adsorption measurement shows that Co/ γ -Al₂O₃ has a high surface of 154 m²/g and a pore volume of 0.57 cm³/g. The Co/Platelet has slightly

higher surface area and pore volume than the Co/Fishbone catalyst, but the values are close. Therefore, the surface areas and pore volumes of Co/CNFs catalysts are lower than that of Co/ γ -Al₂O₃, but higher than that of Co/ α -Al₂O₃ (table 1). The average pore sizes of Co/CNFs catalysts are around 9 nm, which is also close to the pore size of the Co/ γ -Al₂O₃ catalyst. The average pore size of Co/ α -Al₂O₃, however, is much larger (65 nm).

XRD study of the calcined catalysts shows that cobalt exists as Co₃O₄ for all the catalysts. Particle sizes calculated from the Scherrer equation at the most intensive peak of $2\theta = 36.9^\circ$ indicate that the smallest Co₃O₄ particles (16 nm) exist on the platelet CNF (table 1); while on the low surface area α -Al₂O₃, the particle size has the largest value of 43 nm. The Co₃O₄ particle sizes on fishbone CNF and γ -Al₂O₃ are 25 and 19 nm, respectively. The Co₃O₄ particle sizes were converted to the corresponding Co particle sizes according to the relationship $d(\text{Co}^0) = 0.75 \cdot d(\text{Co}_3\text{O}_4)$ [13]. The resulting metallic Co particle sizes are presented in the corresponding parenthesis in table 1.

H₂ chemisorption shows that on the platelet CNF, a relatively high dispersion of 10.1% is achieved, which in fact is recognized as high values for cobalt catalysts prepared by the incipient wetness method [14]. Although the surface area and pore volume of γ -Al₂O₃ is higher than that of platelet CNF, the dispersion achieved on γ -Al₂O₃ is lower than for platelet CNF. The dispersion of Co/Fishbone catalyst is only half of the Co/Platelet value. The lowest dispersion is obtained on the low surface area α -Al₂O₃ with a value of 2.7% (table 2).

Using the formula $d(\text{Co}^0) = 96/D$ [15], where *d* (nm) and *D* (%) are particle size and dispersion, respectively, the particle sizes calculated from the total amount of chemisorbed H₂ show very similar values as the ones measured by XRD (table 1).

It is expected that high surface area supports with a large mesopore volume will lead to high dispersion and small particle sizes of the supported metals. However, even though the surface area and pore volume of the platelet CNF is lower than that of γ -Al₂O₃, the

Table 1
Characterization results of different cobalt catalysts

Catalysts	BET surface area (m ² /g)	Pore volume (cm ³ /g)	Poresize (nm)	Co ₃ O ₄ particle size (nm)		
				XRD ^a	Chemisorption ^b	TEM ^d
Co/ γ -Al ₂ O ₃	154 ^d	0.57 ^d	11.9	19 (14) ^d	14 ^d	
Co/ α -Al ₂ O ₃	9 ^d	0.25 ^{c,d}	65 ^c	43 (32) ^d	35 ^d	
Co/Fishbone	93	0.19	9.2	25 (19)	20	26 (20)
Co/Platelet	113	0.23	9.0	16 (12)	10	16 (12)

^aParticle sizes of Co₃O₄; values in the parentheses are the calculated particle sizes of corresponding metallic cobalt using $d(\text{Co}^0) = 0.75 \cdot d(\text{Co}_3\text{O}_4)$.

^bChemisorption values from the total adsorption of H₂ gives average particle sizes of metallic cobalt.

^cMeasured by mercury intrusion.

^dDetails are given in [19].

Table 2
Reaction rate and turnover frequency of different catalysts

Catalyst	D ^a (%)	$-r_{\text{CO}}^{\text{b}} \cdot 10^2$ (mol CO/(g·h))	TOF ^c · 10 ³ (s ⁻¹)
Co/ γ -Al ₂ O ₃	7.0	3.0	58
Co/ α -Al ₂ O ₃	2.7	1.2	62
Co/Fishbone	4.9	1.5	42
Co/Platelet	10.1	3.3	45

^a Cobalt dispersion based on hydrogen chemisorption (Table 1).

^b The reaction rate of carbon monoxide was obtained at 483 K, 20 bar, and H₂/CO = 2.1 and recorded after 8 h on stream.

^c TOF is calculated as $\text{TOF}_{\text{CO}} = \frac{-r_{\text{CO}} \cdot M_{\text{Co}}}{x_{\text{Co}} \cdot D_{\text{Co}}}$, where $M_{\text{Co}} = 58.9$ g/mol and $x_{\text{Co}} = 0.12$.

dispersion on the platelet CNF is higher than for Co on γ -Al₂O₃. This can be ascribed to the large amount of edge sites associated with the platelet CNFs, which consists mostly of surface carboxyl groups and provides anchoring sites for cobalt particles in addition to the mesoporous structure. This is illustrated on the high resolution TEM image of figure 1(a). On the other hand, for Fischer–Tropsch catalysts the optimum cobalt dispersions have been suggested to be favored by support–precursor combinations with intermediate interaction strength. On strongly interacting supports, high

reduction temperature is required that could lead to sintering; on weakly interacting supports, the supports are unable to stabilize small precursor crystallites during impregnation and drying [15].

It is also interesting to observe that the dispersion of Co/Fishbone is only half of the dispersion of Co/Platelet, even though their surface areas, pore volumes, and pore sizes are not that different. For the fishbone structure, the graphite sheets are oriented at an angle to the fiber axis; while for the platelet structure, the graphite sheets are perpendicular to the fiber axis. Hence, the platelet CNFs only have edge sites exposed, *i.e.*, the relative amount of surface oxygen groups could be more than for fishbone CNF. The platelet CNFs therefore could have more carboxyl groups to stabilize small cobalt precursors which could have contributed to its higher dispersion compared with the fishbone CNF. In addition, it has been suggested that the interaction of the transition metals with the CNFs depends on their curvature [17]. The different structures of platelet and fishbone CNFs probably have different curvatures and thus the interaction strength with cobalt could be different.

TEM characterization has been performed for the calcined CNFs supported catalysts. As shown in figure 1(b) and (c), the Co₃O₄ particles seem to be

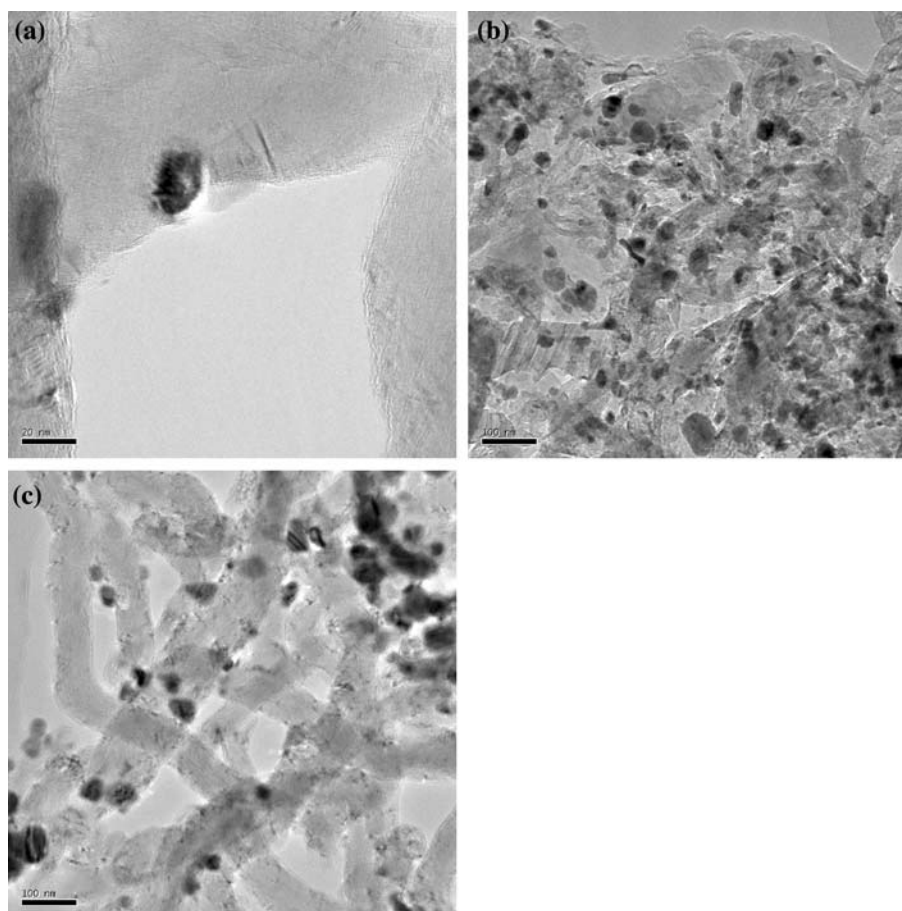


Figure 1. TEM images of (a) a cobalt oxide particle deposited on the edge of a fishbone CNF; (b) Co/Platelet catalyst; (c) Co/Fishbone catalyst.

dispersed homogeneously on the platelet CNF, whereas on the fishbone CNF the particles are not that homogeneously distributed and there are even some quite big particles. This is more clearly shown by the particle size distribution analysis from TEM (figure 2), where about 150 particles have been studied for each sample. The average Co_3O_4 particle sizes determined from the TEM study for Co/Platelet and Co/Fishbone are 16 and 26 nm, respectively, which are consistent with the XRD and chemisorption measurements. The corresponding metallic cobalt particle sizes are also calculated and presented in table 1.

3.2. Activity test

Figure 3 shows the reaction rate for formation of hydrocarbons versus time on stream for the four catalysts. After about 30 h on stream the GHSV has been adjusted in order to compare the catalysts at the same conversion levels. With respect to activity, the samples fall into two groups. The $\gamma\text{-Al}_2\text{O}_3$ and the platelet CNF supported catalysts show higher reaction rate ($\text{g}/(\text{g}_{\text{cat}} \cdot \text{h})$). The reaction rate is initially approximately twice the rate for cobalt supported on $\alpha\text{-Al}_2\text{O}_3$ and fishbone CNF.

It is generally believed that the Fischer–Tropsch synthesis is a structure insensitive reaction [13, 16]. Thus, the activity can be directly correlated to the dispersion of the cobalt particles. With this in mind, it is therefore not surprising that the initial activity follows the order $\text{Co}/\text{Platelet} > \text{Co}/\gamma\text{-Al}_2\text{O}_3 > \text{Co}/\text{Fishbone} > \text{Co}/\alpha\text{-Al}_2\text{O}_3$ since the dispersion is in the same order. The turnover frequencies are summarized in table 2, and it appears that the values for the CNF supports are somewhat lower than for the alumina supports. The turnover frequencies are calculated using the dispersion based on H_2 chemisorption and the measured reaction rate after 8 h on stream. It is evidenced from figure 3 that the rate of deactivation depends on the support, and the CNF supports result in higher deactivation rates and this will influence the turnover frequency. Considering the uncertainties in the measurement of the reaction rates, it is still fair to say

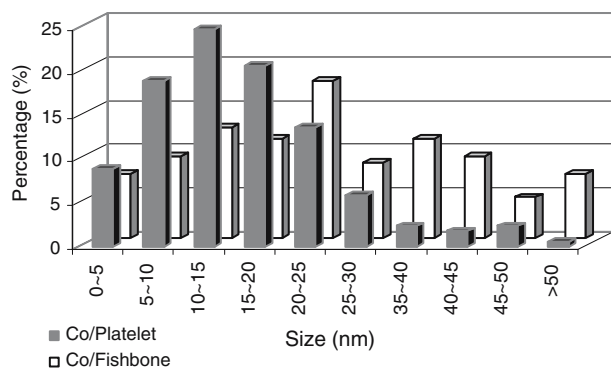


Figure 2. Co_3O_4 particle size distribution of Co/Platelet and Co/Fishbone catalyst from TEM study.

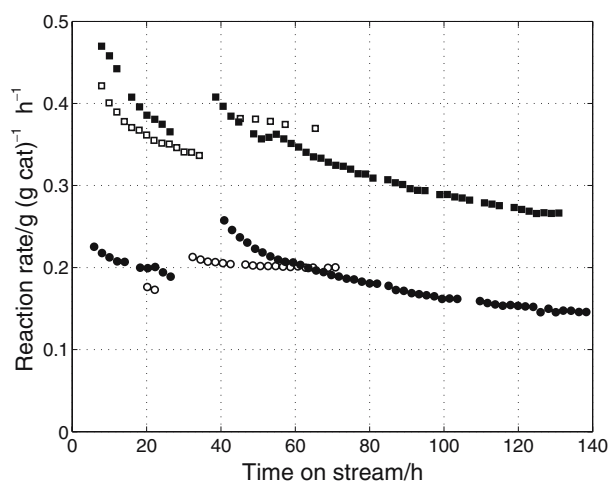


Figure 3. Reaction rates for formation of hydrocarbons at 483 K, 20 bar, and $\text{H}_2/\text{CO} = 2.1$ (■ = Co/Platelet, □ = Co/ $\gamma\text{-Al}_2\text{O}_3$, ● = Co/Fishbone, ○ = Co/ $\alpha\text{-Al}_2\text{O}_3$).

that the turnover frequency is rather similar on the CNF and alumina supports. Therefore, it is at this point inclusive as to whether CNF supports exert any structural effects on the cobalt particles. However, due to the high dispersion easily obtained with the platelet CNF supported catalyst, the initial productivity of the platelet CNF supported catalyst on per gram basis is higher than or comparable to the $\gamma\text{-Al}_2\text{O}_3$ supported catalyst.

Since the product selectivity strongly depends on the conversion, the selectivity of the different catalysts was compared at the same level of conversion rather than at constant space velocity. The selectivity to CH_4 and long-chained hydrocarbons (C_{5+}) at 40% conversion of carbon monoxide is summarized in table 3. The C_{5+} selectivity ranges from 78.7% for Co/ $\gamma\text{-Al}_2\text{O}_3$ to 82.5% for Co/ $\alpha\text{-Al}_2\text{O}_3$. The C_{5+} selectivity obtained with Co/Platelet can almost compete with the high value for the $\alpha\text{-Al}_2\text{O}_3$ supported catalyst. The Co/Fishbone catalyst also exhibits selectivity higher than that of $\gamma\text{-Al}_2\text{O}_3$. The high selectivity to C_{5+} of low surface $\alpha\text{-Al}_2\text{O}_3$ has partly been explained by the reduced activity for secondary hydrogenation of olefins, and is further correlated with the surface area, pore volume, or pore diameter of the support [18]. However, in this study no such correlations with the selectivity can be found and the results indicate that

Table 3
Selectivity at 40% CO conversion ($T = 483 \text{ K}$, $P = 20 \text{ bar}$, $\text{H}_2/\text{CO} = 2.1$)

Catalyst	GHSV ($\text{l}/(\text{g cat} \cdot \text{h})$)	Selectivity (%)	
		C_{5+}	CH_4
Co/ $\gamma\text{-Al}_2\text{O}_3$	3.4	78.7	10.3
Co/ $\alpha\text{-Al}_2\text{O}_3$	3.1	82.5	8.9
Co/Fishbone	2.6	81.0	10.6
Co/Platelet	4.1	81.6	10.9

the selectivity to C_{5+} depends on both the pore structure and the support identity. At this moment the reason for the high selectivity of CNFs is not clear. One possible explanation is that the CNFs are free of micropores and exert less transport limitation for the reactants and products, similar as the macropore-containing α - Al_2O_3 .

Our initial study by steady-state isotopic transient kinetic analysis (SSITKA) has shown that the adsorption ratio of CO/H_2 is always higher on CNFs supported cobalt catalysts than on alumina supported cobalt [19], which could also be one possible reason for the high selectivity to C_{5+} for CNFs.

4. Conclusions

Cobalt supported on carbon nanofibers with a special platelet structure can easily achieve high dispersion, probably because of a high number of edge sites, and thus also surface oxygen groups. The platelet CNF combines two attractive features of the alumina supports, namely the high activity of γ - Al_2O_3 and the high C_{5+} selectivity of α - Al_2O_3 . Reaction rates determined at 483 K, 20 bar, and $H_2/CO = 2.1$, together with selectivity to long-chained hydrocarbons (C_{5+}), have shown that platelet CNFs could be interesting supports for the Fischer–Tropsch synthesis. Further investigations are underway to identify the metal–CNF interactions and to possibly improve the activity, selectivity, and stability of platelet CNF supported cobalt Fischer–Tropsch catalysts.

Acknowledgment

The financial support from Statoil and the Norwegian Research Council (NFR) is greatly acknowledged.

References

- [1] S. Storsæter, Ø. Borg, E.A. Blekkan and A. Holmen, *J. Catal.* 231 (2005) 405.
- [2] G. Jacobs, T.K. Das, Y. Zhang, J. Li, G. Racoillet and B.H. Davis, *Appl. Catal. A* 233 (2002) 263.
- [3] R. Oukaci, A.H. Singleton and J.G. Goodwin Jr., *Appl. Catal. A* 186 (1999) 129.
- [4] E. Iglesia, S.L. Soled, J.E. Baumgartner and S.C. Reyes, *J. Catal.* 153 (1995) 108.
- [5] Ø. Borg, S. Storsæter, E.A. Blekkan, S. Eri, E. Rytter and A. Holmen, in preparation.
- [6] S. Eri, K.J. Kinnari, D. Schanke and A.M. Hilmen, U.S. Patent 2004/0077737 A1.
- [7] P. Serp, M. Corrias and P. Kalck, *Appl. Catal. A* 253 (2003) 337.
- [8] M.C. Bahome, L.L. Jewell, D. Hildebrandt, D. Glasser and N.J. Coville, *Appl. Catal. A* 287 (2005) 60.
- [9] G.L. Bezemer, A. van Laak, A.J. van Dillen and K.P. de Jong, *Stud. Surf. Sci. Catal.* 147 (2004) 259.
- [10] Z. Yu, D. Chen, B. Tøtdal and A. Holmen, *J. Phys. Chem. B* 109 (2005) 6096.
- [11] A.-M. Hilmen, E. Bergene, O.A. Lindvåg, D. Schanke, S. Eri and A. Holmen, *Catal. Today* 105 (2005) 357.
- [12] B. Chr. Enger, V. Frøseth, Ø. Borg, E. Rytter and A. Holmen, in preparation.
- [13] D. Schanke, S. Vada, E.A. Blekkan, A.M. Hilmen, A. Hoff and A. Holmen, *J. Catal.* 156 (1995) 85.
- [14] C.M. Lok, *Stud. Surf. Sci. Catal.* 147 (2004) 283.
- [15] R.C. Reuel and C.H. Bartholomew, *J. Catal.* 85 (1984) 63.
- [16] E. Iglesia, *Appl. Catal. A* 161 (1997) 59.
- [17] M. Menon, A.N. Andriotis and G.E. Froudakis, *Chem. Phys. Lett.* 320 (2000) 425.
- [18] D. Schanke, S. Eri, E. Rytter, C. Aaserud, A.M. Hilmen, O.A. Lindvåg, E. Bergene and A. Holmen, *Stud. Surf. Sci. Catal.* 147 (2004) 301.
- [19] V. Frøseth, Z. Yu, D. Chen and A. Holmen, in preparation.